

# Structural control of the non-ionic surfactant alcohol ethoxylates (AEOs) on transport in natural soils

M. Botella Espeso<sup>1</sup>, C. Corada-Fernández<sup>2</sup>, M. García-Delgado<sup>2</sup>, L. Candela<sup>3</sup>,  
E. González-Mazo<sup>2</sup>, P.A. Lara-Martín<sup>2</sup>, J. Jiménez-Martínez<sup>1,4\*</sup>

<sup>1</sup> Department of Civil, Environmental and Geomatic Engineering, ETH Zurich, 8093 Zürich, Switzerland

<sup>2</sup> Department of Physical Chemistry, Faculty of Marine and Environmental Sciences, University of Cadiz, Campus of International Excellence of the Sea (CEI•MAR), Río San Pedro, Puerto Real, Cadiz 11510, Spain

<sup>3</sup> IMDEA Water, Avenida Punto Com 2, Parque Científico Tecnológico de la Universidad de Alcalá, Alcalá de Henares, 28805 Madrid, Spain

<sup>4</sup> Department of Water Resources and Drinking Water, Eawag, 8600 Dübendorf, Switzerland

\*Corresponding author: [joaquin.jimenez@eawag.ch](mailto:joaquin.jimenez@eawag.ch) / [jjimenez@ethz.ch](mailto:jjimenez@ethz.ch)

**ABSTRACT.** Surfactants, after use, enter the environment through diffuse and point sources such as irrigation with treated and non-treated waste water and urban and industrial wastewater discharges. For the group of non-ionic synthetic surfactant alcohol ethoxylates (AEOs), most of the available information is restricted to the levels and fate in aquatic systems, whereas current knowledge of their behavior in soils is very limited. Here we characterize the behavior of different homologs (C12–C18) and ethoxymers (EO3, EO6, and EO8) of the AEOs through batch experiments and under unsaturated flow conditions during infiltration experiments. Experiments used two different agricultural soils from a region irrigated with reclaimed water (Guadalete River basin, SW Spain). In parallel, water flow and chemical transport were modelled using the HYDRUS-1D software package, calibrated using the infiltration experimental data. Estimates of water flow and reactive transport of all surfactants were in good agreement between infiltration experiments and simulations. The sorption process followed a Freundlich isotherm for most of the target compounds. A systematic comparison between sorption data obtained from batch and infiltration experiments revealed that the sorption coefficient ( $K_d$ ) was generally lower in infiltration experiments, performed under environmental flow conditions, than in batch experiments in the absence of flow, whereas the exponent ( $\beta$ ) did not show significant differences. For the low clay and organic carbon content of the soils used, no clear dependence of  $K_d$  on them was observed. Our work thus highlights the need to use reactive transport parameterization inferred

38 under realistic conditions to assess the risk associated with alcohol ethoxylates in subsurface  
39 environments.

40

41 **Main findings:** AEOs sorption coefficients were lower and with less variability in infiltration than  
42 batch experiments. Similar behaviour in natural systems between homologs and between  
43 ethoxymers. No dependence of sorption coefficient on low clay and organic carbon content.

44

## 45 **1. Introduction**

46

47 Surfactants are among the most widely used synthetic chemicals globally, with applications in the  
48 formulation of pesticides, paints, pharmaceuticals, wetting agents, pulp and paper industries, and  
49 personal care products, among many others, but their main use is in the formulation of domestic  
50 and industrial detergents. After use, surfactants enter the environment through diffuse, *e.g.*, runoff,  
51 and point sources, mainly from urban and industrial wastewater discharges. Although the removal  
52 rate of most these compounds during wastewater treatment is often very high (95–99%; Matthijs  
53 et al., 1999; McAvoy et al., 1998), they can reach terrestrial environments through irrigation using  
54 reclaimed water or application of sludge as fertilizer in agriculture (Topp et al., 2012). As a result  
55 of their widespread and high volume of use, surfactants have been detected in a variety of  
56 continental and marine aquatic systems (González-Mazo et al., 1998, 2002; León et al., 2001).  
57 Most of the studies focused on the anionic linear alkylbenzene sulfonates (LAS) (Eichnorn et al.,  
58 2002; Carlsen et al., 2002; Ding et al., 1999) and the non-ionic alkylphenol ethoxylates (APEOs)  
59 (Jonkers et al., 2003; Ferguson et al., 2001). Their presence and fate in subsurface environments  
60 have received been widely studied. In aquifers, the degradation of alkylphenol ethoxylates has  
61 been detected, producing ethoxycarboxylated alkylphenols and alkylphenols (Ahel et al., 1996;  
62 Montgomery-Brown et al., 2003; Guang-Guo, 2006; Tubau et al., 2010), which are estrogenic.  
63 The presence of sulfophenyl carboxylic acids derived from linear alkylbenzene sulfonate degradation  
64 has also been detected in groundwater (Krueger et al., 1998; Tubau et al., 2010). However, the  
65 characterization of their percolation has received less attention. Percolation experiments performed  
66 for LAS shown that their retention was favored by higher clay and organic matter contents  
67 (McAvoy et al., 1994; Küchler and Schnaak, 1997; Boluda et al., 2010). In the case of  
68 biodegradation within the soil column, > 25% of LAS was removed, reducing percolation to deeper

69 layers.

70

71 Here we focus on alcohol ethoxylates (AEOs), which are another important group of non-ionic  
72 surfactants that are commonly used in domestic and commercial detergents, household cleaners  
73 and personal care products (Droge and Hermens, 2007; Hermens and Droge, 2009). AEOs are  
74 efficiently removed (up to 99%) in wastewater treatment plants by a combination of sorption onto  
75 sludge and aerobic degradation (Szymanski et al., 2003; Wind et al., 2006), with total AEO  
76 concentrations in the effluents ranging from 0.92 to 22.7  $\mu\text{g/L}$  in Europe and North America  
77 (Eadsforth et al., 2006; Morrall et al., 2006). Once in the environment, their behavior is controlled  
78 by further sorption and degradation processes. AEOs are found dissolved and associated with  
79 particulate material, with previous field measures suggesting that up to 86% of the total measured  
80 concentration is found sorbed on suspended solids (Lara-Martín et al., 2008). Partition coefficients  
81 have been measured ranging from 40 to 7,000 L/kg (Cano and Dorn, 1996; Kiewiet et al., 1996;  
82 Van Compernelle et al., 2006; Droge et al., 2009), depending on the polarity and sorption capacity  
83 of the different AEO homologs and ethoxymers. Most of these studies characterized the sorption  
84 of these surfactants using very high concentrations, of several ppm (up to 2,000 ppm) (Podoll et  
85 al., 1987). However, in the environment, these chemicals are found at much lower concentrations,  
86 *e.g.*, in the water column they are usually in the low ppb range (Lara-Martín et al., 2011).  
87 Furthermore, most of the available information is restricted to the levels and fate of AEOs in  
88 aquatic systems (Petrovic et al., 2002; Lara-Martín et al., 2005, 2008, 2014; Corada-Fernández et  
89 al., 2011, 2013). Natural abatement of AEOs occur in terrestrial environments due to a  
90 combination of biodegradation and sorption, delaying the arrival of these contaminants in aquifers  
91 and minimizing, but not eliminating (García et al., 2019), the risk of groundwater pollution (Durán-  
92 Álvarez et al., 2014; Corada-Fernández et al., 2017). However, current knowledge of their  
93 behavior in soils is limited. Some of the works carried out in soils have been mainly focus on the  
94 ability of non-ionic surfactants to solubilize relatively insoluble contaminants such as  
95 hydrocarbons (*e.g.*, Lee et al., 2000; Haigh, 1996). The sorption of non-ionic surfactants in soils  
96 have been characterized for following a Langmuir isotherm (Lee et al., 2005) and two-sorption  
97 regimes (Adeel and Luthy, 1995). A competition between AEOs homologs for adsorption sites has  
98 also been described (Droge and Hermens, 2010). A high correlation with soil mineral properties  
99 has been observed (Lee et al., 2005), as well as a much greater role of the chain length of AEOs in

100 the interaction (association) with humic substances as compared to the ethoxylate group member  
101 (McAvoy and Kerr, 2001).

102  
103 Understanding the coupling of natural abatement and transport of AEOs in soils is determinant for  
104 predicting their mobility and leaching to groundwater. We here describe laboratory experiments  
105 to quantify the fate and transport of AEOs in two natural soils, using a variety of AEOs to represent  
106 the wide structural diversity of commercial products, which include compounds with different  
107 numbers of carbon atoms in their hydrophobic alkyl chain bonded to a hydrophilic chain with a  
108 varying number of ethoxylate units. By combining batch and infiltration experiments, we are able  
109 to compare parameters estimated in the absence of flow in batch experiments, with those obtained  
110 under realistic environmental flow conditions in infiltration experiments. The use of a numerical  
111 solver to simulate the non-equilibrium chemical transport of the targeted compounds allowed us  
112 to parameterize the sorption of AEOs under real environmental conditions.

113

## 114 **2. Materials and methods**

115

### 116 **2.1. Characterization of soil samples**

117 Soil samples were taken from two locations, locally known as Rio Viejo (soil core 1) and  
118 Guadalcaçín (soil core 2), in a region where agricultural soils are irrigated with reclaimed water  
119 and amended using sludge, after being composted (Guadalete River basin, SW Spain) (Biel-Maeso  
120 et al., 2017). Soil physical properties were determined with respect to depth using a series of  
121 techniques and standards (Table 1). The grain size distribution was determined according to ASTM  
122 D 422-63 and Gee and Or (2002). Soil textural class was defined according to the USDA system.  
123 Bulk density was determined following Grossman and Reinsch (2002). Saturated hydraulic  
124 conductivity, which can be highly affected by the concentration of surfactants in the solution, was  
125 empirically determined in the laboratory (Reynolds and Elrick, 2002). Organic carbon (OC)  
126 content was determined by dichromate oxidation, following Gaudette et al. (1974) and the  
127 modification proposed by El Rayis (1985).

128

### 129 **2.2. Infiltration experiments**

130 Infiltration experiments were performed in *quasi* two-dimensional flow cells (495 mm × 587 mm

131  $\times 10$  mm, see Figure 1). One flow cell was filled for each soil sample, maintaining the natural  
132 order and thickness of their horizons and the original bulk density (Table 1). The base of each flow  
133 cell was filled with silica sand (Ottawa sand) to ensure drainage. Infiltration experiments lasted  
134 192 hours for soil core 1, and 69 hours for soil core 2, and were conducted at constant temperature  
135 (20 °C). An AEO solution consisting of a mixture of homologs (C12, C14, C16, and C18) and their  
136 corresponding ethoxymers (3, 6 and 8 EO ethoxylated groups) (Sigma-Aldrich) at 100 ng/cm<sup>3</sup> (100  
137 ppb) was injected for the duration of the experiments at a constant flow rate (0.083 and 0.43 cm<sup>3</sup>/h  
138 for soil 1 and 2, respectively) using a peristaltic pump and an evenly drip irrigation system. The  
139 goal is to characterize the general behavior of AEOs and the control of their structural diversity  
140 under different environmental conditions, including flow conditions and soil types, rather than a  
141 systematic comparison between soil types. The applied concentration of AEOs mimics previously  
142 recorded environmental conditions. The applied solution contained the same concentration of  
143 cations (SAR = 5.31) as the original interstitial water of the soil, with pH [8 – 8.3], electrical  
144 conductivity [500 – 800]  $\mu$ S/cm, and cation-exchange capacity [32 – 35] mmol/kg (Corada-  
145 Fernandez et al., 2015). Soil and water samples were collected at the same depths throughout the  
146 profile of the flow cell before and after the experiments in order to characterize the mobility of the  
147 targeted compounds. The concentration of AEOs in both phases was analyzed following Lara-  
148 Martin et al. (2012), providing measures of water content and total concentrations (sorbed +  
149 dissolved) of the contaminants at each selected depth.

150

151

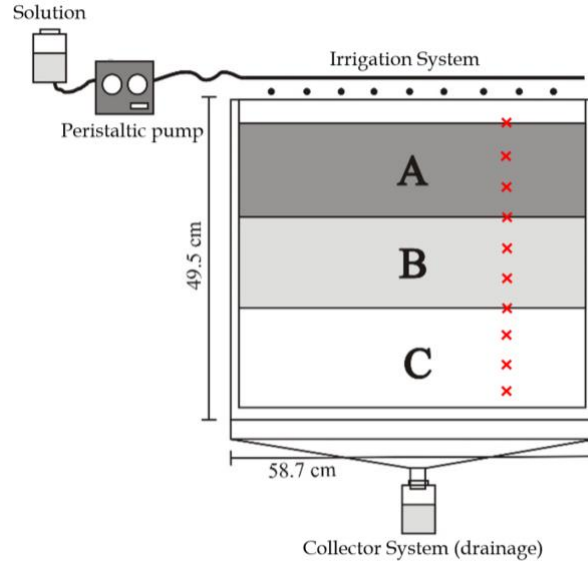


**Figure 1.** Schematic of the flow cell for the infiltration experiments. A drip irrigation system provided a solution containing a mixture of AEOs at a constant flow rate throughout the experiments. The collector system provided drainage. Soil horizons (shading) and sample points (crosses) are shown for soil core 1.

152

153

154 **Table 1.** Physico-chemical and hydraulic properties of soil cores 1 and 2. OC is the soil organic  
 155 carbon content;  $\rho_b$  is the bulk density;  $\theta_r$ , and  $\theta_s$  are the residual and saturated water content,  
 156 respectively;  $\alpha$  is the inverse of the air entry value;  $n$  is the pore size distribution index;  $K_s$  is the  
 157 saturated hydraulic conductivity; and  $\lambda$  is the dispersivity of solute in each soil horizon.

Horizon	Depth [cm]	Texture [%]			OC [%]	$\rho_b$ [g/cm <sup>3</sup> ]	Soil type	$\theta_r$ [cm <sup>3</sup> /cm <sup>3</sup> ]	$\theta_s$ [cm <sup>3</sup> /cm <sup>3</sup> ]	$\alpha$ [1/cm <sup>1</sup> ]	$n$ [-]	$K_s$ [cm/h]	$\lambda$ [cm]
		Sand	Silt	Clay									
1A	0–19	41.71	54.68	3.61	1.1	1.3349	Silty loam	0.0343	0.3638	0.0091	1.5477	2.67	0.6
1B	19–30.5	84.42	14.58	1	0.3	1.5154	Loamy sand	0.0392	0.3739	0.0436	2.1783	8.97	1.87
1C	30.5–47.1	100	0	0	0	1.9438	Sand	0.049	0.2663	0.0295	4.036	26.23	1.3
2A	0–14	64.36	33.29	2.35	1.2	1.6499	Sandy loam	0.0277	0.3639	0.0507	1.3946	1.50	2.37
2B	14–18.5	46.4	51.88	1.72	0.6	1.6868	Silt loam	0.0252	0.427	0.0319	1.3423	0.95	3.04
2C	18.5–29.5	41.17	54.77	4.06	0.6	1.7095	Silt loam	0.0277	0.3557	0.0245	1.3515	0.66	3.04
2D	29.5–46.5	100	0	0	0	2.0098	Sand	0.0492	0.2563	0.0288	4.1103	23.62	1.3

158

159

160

161 **2.3. Batch experiments**

162 Sorption isotherms were determined using conventional batch experiments following the OECD  
163 106 guidelines, as previously reported for characterizations of the sorption of AEOs onto marine  
164 sediments (Travero-Soto et al., 2014). Briefly, for each soil horizon, 0.5 g of freeze-dried soil were  
165 placed in 80 mL polypropylene tubes and stirred together with 50 mL of sterilized water containing  
166 different concentrations of AEO homologs (C12, C14, C16, and C18) and their corresponding  
167 ethoxymers (3, 6 and 8 EO ethoxylated groups) (5, 10, 25, 50, 100, and 200 ng/cm<sup>3</sup>) for 24 h. The  
168 aqueous phase was separated from the soil by centrifugation (30 min at 20,000g) and analyzed  
169 following Lara-Martin et al. (2012). Sorption of AEOs by the particulate phase was quantified as  
170 the difference between the initial concentration in solution and that measured at the end of the  
171 experiment. Control experiments were also performed to check for the biodegradation of AEO  
172 homologs, the sorption to the walls of the containers used, and the possible contribution of soils to  
173 the mass of AEO added, resulting all of them being negligible (< 1%).

174

175 **2.4. Modelling reactive transport**

176 To simulate the water flow and reactive transport of the AEO homologs and ethoxymers during  
177 the infiltration experiments, the HYDRUS-1D code was used (Šimůnek et al., 2015). Flow and  
178 transport equations described below are solved by the software numerically using standard  
179 Galerkin-type linear finite element schemes subjected to appropriate initial and boundary  
180 conditions (Šimůnek et al., 2015).

181

182 **2.4.1. Variably saturated flow**

183 For uniform one-dimensional flow in a partially saturated porous medium, and assuming that the  
184 gas phase does not play a significant role in the flow of the liquid phase, the equation governing  
185 the flow is given by the following modified Richards expression:

186

$$187 \quad \frac{\partial \theta}{\partial t} = \frac{\partial}{\partial x} \left[ K \left( \frac{\partial h}{\partial x} + 1 \right) \right] - S, \quad (1)$$

188

189 where  $\theta$  is the volumetric water content [L<sup>3</sup> L<sup>-3</sup>],  $h$  the soil pressure head [L],  $S$  the sink term [T<sup>-1</sup>],  
190  $x$  the spatial coordinate in the vertical direction [L], and  $t$  the time [T].  $K$  is the unsaturated  
191 hydraulic conductivity [L T<sup>-1</sup>], and is as follows:

192  
193  
194  
195  
196  
197  
198  
199  
200  
201  
202  
203  
204  
205  
206  
207  
208  
209  
210  
211  
212  
213  
214  
215  
216  
217  
218  
219

$$K(h, z) = K_s(x)K_r(h, x), \quad (2)$$

where  $K_r$  is the relative hydraulic conductivity and  $K_s$  the saturated hydraulic conductivity [ $L T^{-1}$ ].

Water retention and unsaturated hydraulic conductivity functions of each soil layer were obtained from the constitutive equation of van Genuchten–Mualem (Mualem, 1976; van Genuchten, 1980)

$$\theta(h) = \begin{cases} \theta_r + \frac{\theta_s - \theta_r}{[1 + |\alpha h|^n]^{1-1/n}} & h < 0 \\ \theta_s & h \geq 0 \end{cases} \quad (3)$$

$$K(h) = K_s S_e^l \left\{ 1 - \left[ 1 - S_e^{n/(n-1)} \right]^{1-1/n} \right\}^2, \quad (4)$$

where  $S_e$  is the effective saturation

$$S_e = \frac{\theta(h) - \theta_r}{\theta_s - \theta_r} \quad (5)$$

and  $\theta(h)$  the volumetric water content at pressure head  $h$ , *i.e.*, water retention function. The parameters  $\theta_r$  and  $\theta_s$  are the residual and saturated water content, respectively,  $\alpha$  is the inverse of the air entry value,  $n$  is the pore size distribution index, and  $l$  is a pore-connectivity parameter. In order to reduce the number of parameters,  $l$  is commonly assumed to be 0.5, *e.g.*, Mualem (1976). Initial values of these parameters were estimated using ROSETTA (Schaap et al., 2001), a pedotransfer function model that predicts hydraulic parameters from soil texture (% of sand, silt, and clay) and related data. In this case, we also consider the soil bulk density,  $\rho_b$  (Table 1).

### 2.4.2. Reactive transport

The transport equation, including the advection-dispersion processes, and degradation and sorption as reactive processes:



220 
$$\frac{\partial \theta C_w}{\partial t} + \frac{\partial \rho_b C_s}{\partial t} = \frac{\partial}{\partial x} \left( \theta D \frac{C_w}{\partial x} \right) - \frac{\partial q C_w}{\partial x} - \mu \theta C_w, \quad (6)$$

221  
 222 where  $C$  is the chemical concentration [ $M L^{-3}$ ], with subscripts  $w$  and  $s$  for the concentration in the  
 223 interstitial water and sorbed in the solids, respectively;  $q$  is the water flux [ $LT^{-1}$ ];  $\mu$  is the  
 224 degradation constant for the chemical in liquid phase [ $T^{-1}$ ]; and  $\rho_b$  is the bulk density of the soil  
 225 [ $M L^{-3}$ ].  $D$  is the dispersion coefficient [ $L^2 T^{-1}$ ] following Bear (1972):

226  
 227 
$$\theta D = \lambda |q| + \theta D_m \tau_w, \quad (7)$$

228  
 229 where  $D_m$  is the molecular diffusion coefficient [ $L^2 T^{-1}$ ];  $\tau_w$  is the tortuosity, computed as  $\tau_w =$   
 230  $\theta^{7/3} / \theta_s^2$  following Millington and Quirk (1961);  $|q|$  is the absolute value of flux [ $L T^{-1}$ ]; and  $\lambda$  the  
 231 longitudinal dispersivity [ $L$ ].

232  
 233 The isotherm of sorption that relates  $C_s$  and  $C_w$  is defined as

234  
 235 
$$C_s = \frac{K_d C_w^\beta}{1 + \eta C_w^\beta}, \quad (8)$$

236  
 237 where  $K_d$  [ $L^3 M^{-1}$ ],  $\beta$  [-] and  $\eta$  [ $L^3 M^{-1}$ ] are the coefficients of the isotherm. The isotherms of  
 238 Freundlich, Langmuir and the linear isotherm are specific cases: with  $\beta = 1$  the isotherm is that of  
 239 Langmuir, with  $\eta = 0$  the isotherm is that of Freundlich, while with both  $\beta = 1$  and  $\eta = 0$  the  
 240 isotherm is linear.

241  
 242 **2.4.3. Scaling of the hydraulic properties**

243 The effect of changes in concentration on surface tension and viscosity, and consequently on water  
 244 retention (pressure–water saturation) and hydraulic conductivity functions, were considered using  
 245 Smith and Gillham’s (1994, 1999) scale relationships. From the capillary pressure–surface tension  
 246 ratio, the effect of a solution on the pressure–saturation ratio can be predicted from the relationship  
 247 between the surface tension of pore water as a function of concentration ( $\sigma$ ) and the surface tension  
 248 for pure water ( $\sigma_0$ )

249

250

$$\mathbf{h}(\theta, C_w) = \frac{\sigma}{\sigma_o} h(\theta, C_{w0}), \quad (9)$$

251

252 where  $h(\theta, C_{w0})$  is the pressure for a water content and a reference concentration  $C_{w0}$  ( $C_{w0}$  is 0 for  
253 pure water), and  $\mathbf{h}(\theta, C_w)$  is the soil pressure head scaled to the same water content and  
254 concentration.

255

256 The hydraulic conductivity as a function of concentration  $\mathbf{K}(\theta, C_w)$  is computed from the relation  
257 between viscosity of the solution and pure water as

258

259

$$\mathbf{K}(\theta, C_w) = \frac{\nu}{\nu_o} K(\theta, C_{w0}), \quad (10)$$

260

261 where  $\mathbf{K}(\theta, C_w)$  is the concentration-dependent unsaturated hydraulic conductivity obtained from  
262 the hydraulic conductivity for pure water at the same water content  $K(\theta, C_{w0})$  and according to the  
263 relative viscosity  $\nu/\nu_o$ ,  $\nu$  is the viscosity of pore water as a function of concentration and  $\nu_o$  is the  
264 viscosity for pure water.

265

#### 266 **2.4.4. Modelling setup: initial and boundary conditions**

267

268

269

270

271

272

273

274

275

276

277

278

The flow cells used for infiltration experiments were discretized with 90 equidistant nodes separated by 0.5 cm. Three and four different layers were considered for soil core 1 and 2, respectively, while the mass balance was defined for the whole system. Each soil horizon was assigned an initial water content and concentration of the homologues (C12, C14, C16, and C18) and their corresponding ethoxymers (3, 6 and 8 EO ethoxylated groups). We assumed no hysteresis in the water retention functions. As boundary conditions for the water flow, constant flow at the surface ( $q = 0.083$  mL/min and  $q = 0.43$  mL/min for soil core 1 and 2, respectively) and free drainage at the bottom were imposed. No evaporation was considered at the upper limit. For transport, variable concentration and free drainage were assumed at the upper and lower limit, respectively. A direct simulation was performed to solve unsaturated flow in both infiltration experiments. The inverse method was applied to parameterize the reactive transport processes, in particular the sorption process ( $K_d$ ,  $\beta$  and  $\eta$ , Eq. 8), and compare the values obtained under actual

279 infiltration conditions with those inferred from batch experiments.

280  
281 The parameterization of the reactive transport of the AEOs was completed with the dispersivity  
282 ( $\lambda$ ) for each soil horizon, which was obtained from the literature for the same texture and scale,  
283 *i.e.*, soil horizon thickness (Table 1) (Vanderborght and Vereecken, 2007). The same molecular  
284 diffusion coefficient  $D_m = 1.008 \times 10^{-2}$  cm<sup>2</sup>/h (Song et al., 2006) was used for all contaminants,  
285 and a degradation constant  $\mu$  (1/h) for each of them (Hermens and Droge, 2009) (Table 2). The  $\mu$   
286 values used were slightly higher (*i.e.*, shorter half-life) than the ones provided for similar  
287 compounds (*e.g.*, linear alcohol ethoxylates) in a large variety of soils (Knaebel et al., 1990;  
288 Federle et al., 1997), although within the same order of magnitude. Note that for the numerical  
289 simulations  $\mu$  includes natural decay and biodegradation. The first order sorption rate coefficient  
290 ( $k$ ) for one site or two sites non-equilibrium sorption, *i.e.*, the mass transfer coefficient for solute  
291 exchange between mobile and immobile liquid regions, was estimated as having an average value  
292 of  $k = 6.5$  1/h, with a small variability between surfactants; therefore, the same value was used for  
293 all of them.

294  
295 **Table 2.** Degradation constant  $\mu$  of the alcohol ethoxylates used in the experiments (from Hermens  
296 and Droge, 2009).

Hydrocarbon chain	EO group	$\mu$
		[1/h]
C12	EO3	0.1733
	EO6	0.0866
	EO8	0.0578
C14	EO3	0.1733
	EO6	0.0866
	EO8	0.0866
C16	EO3	0.1733
	EO6	0.0866
	EO8	0.0866
C18	EO3	0.0866
	EO6	0.1733
	EO8	0.1733

297  
298 The transport regime was characterized by two dimensionless numbers, the Péclet number and the  
299 Damköhler number. The Péclet number (Pe) represents the relative importance of advective ( $\tau_a$ )  
300 and diffusive ( $\tau_d$ ) effects during transport. Here, we compute it as  $Pe = \tau_d/\tau_a = (u/D_m)\Delta x$  (El-

301 Kadi and Ge, 1993), where  $u$  is the mean water velocity ( $u = q/\theta$ ), and  $\Delta x$  the spatial  
302 discretization (0.5 cm in this case). The relative importance of transport to chemical reactions is  
303 measured by the Damköhler number ( $Da$ ), representing the ratio of advection ( $\tau_a$ ) to reaction ( $\tau_r$ )  
304 timescales,  $Da = \tau_a/\tau_r$ . The reaction timescale is defined by the kinetics of sorption ( $k$ ) in well-  
305 mixed conditions  $\tau_r = 1/(C_{wo} k)$  (Connors 1990). Chemical reactions can thus be classified as  
306 mixing-driven (or mixing-limited), when the reaction is fast compared to advection ( $Da \gg 1$ ), or  
307 kinetics-driven ( $Da \ll 1$ ).

308

### 309 **3. Results**

310

#### 311 **3.1. Model calibration: flow and reactive transport**

312 Simulations using HYDRUS-1D with the ROSETTA initial hydraulic parameter estimates yielded  
313 water content profiles for both soil cores in the infiltration experiments that were in good  
314 agreement with the experimental data (Figure 2). Transitions between soil horizons are clearly  
315 identified with abrupt changes in water content. The use of parameter optimization routines of  
316 HYDRUS-1D to calibrate the soil hydraulic parameters did not improve the goodness-of-fit of the  
317 direct simulations. The influence of surfactant structures on the equilibrium surface properties, and  
318 sorption behaviors at the air–water interface have been investigated systematically (Kanokkarn et  
319 al., 2017). At very low concentrations, AEOs are maintained almost at the same surface tension  
320 equilibrium level as pure water. For the surfactant concentration used in these experiments, the  
321 impact on surface tension is negligible. Consequently, no changes in the hydraulic properties by  
322 the presence of surfactants were considered.

323

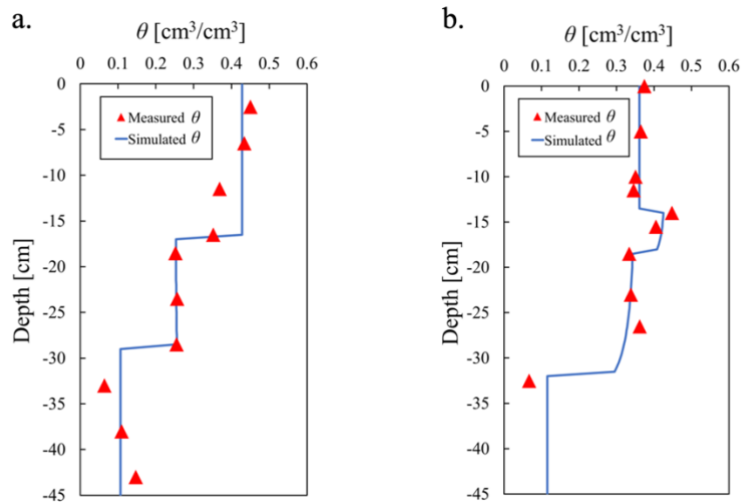


**Figure 2.** Soil water content  $\theta$  [ $\text{cm}^3/\text{cm}^3$ ] with depth measured in the infiltration experiments (triangles) and simulated using HYDRUS-1D with the ROSETTA hydraulic parameter estimates (solid line). Values are shown for soil core 1 (a) and soil core 2 (b), 192 and 69 hours, respectively, after the start of the experiments.

324

325 The set of hydraulic parameters was subsequently used to parametrize, using optimization routines  
 326 of HYDRUS-1D, the isotherm of sorption (Eq. 8) for each surfactant in each soil horizon. The  
 327 average  $Pe$  and  $Da$  were both less than 1, so that an equilibrium or quasi-equilibrium model was  
 328 assumed, *i.e.*, the sorption process was considered to be a fast-reversible reaction. The reactive  
 329 transport of the twelve targeted AEOs in each flow cell was simulated to characterize their sorption  
 330 under realistic conditions. Figure 3 shows a final total concentration ( $C_s + C_w$ ) profile for  
 331 C14AEO8 as an example. Profiles for the other compounds are shown in Figure S1 and S2,  
 332 Supplementary Material.

333

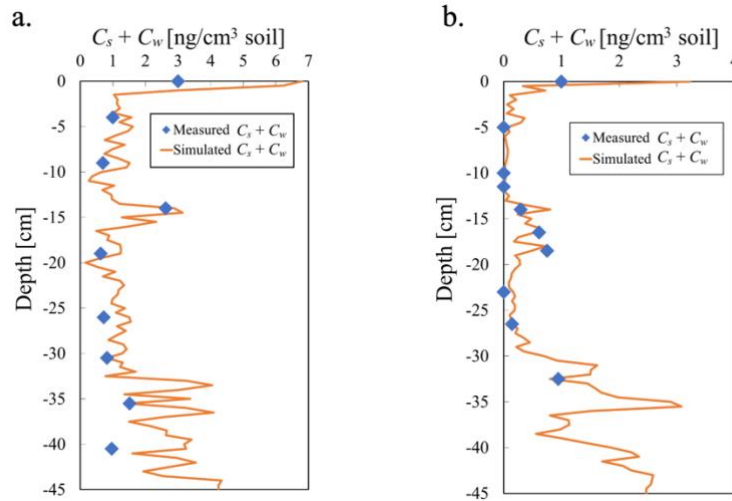


**Figure 3.** Total concentration ( $C_s + C_w$ ) [ $\text{ng}/\text{cm}^3$  of soil] of C14AEO8 measured at different depths in the infiltration experiments (rhomboids) and simulated using HYDRUS-1D (solid line). Values are shown for soil core 1 (a) and soil core 2 (b), 192 and 69 hours, respectively, after the start of the experiments.

334

335 Overall, there was good agreement between the measured concentrations at the different depths in  
 336 the infiltration experiments and the HYDRUS-1D predictions at the same depths (Table 3). The  
 337 use of the coefficient of determination ( $R^2$ ) was discarded because it is insensitive to additive and  
 338 proportional differences between the model simulations and observations, *i.e.*, large values of  $R^2$   
 339 can be obtained even when the model-simulated values differs considerably in magnitude and  
 340 variability from the observed ones. Instead, a dimensionless measure, the coefficient of efficiency  
 341 ( $E$ ), also called Nash-Sutcliffe model efficiency coefficient (Nash and Sutcliffe, 1970), can provide  
 342 a relative assessment of the model performance. The root mean square error ( $RMSE$ ) was  
 343 systematically greater than the mean absolute error ( $MAE$ ), indicating the presence of outlier  
 344 values. As a consequence, we employ a modified coefficient of efficiency ( $E'$ ), in which the errors  
 345 and differences (between measured and simulated) are given their appropriate weighting, rather  
 346 than being inflated by their squared values (Legates and McCabe, 1999; Ritter and Muñoz-  
 347 Carpena, 2013). The criteria is as follow:  $E' = 1$  when the model fits the data perfectly;  $E' = 0$   
 348 when the model provides predicted values that are as accurate as using the mean of the  
 349 observations; and  $E' < 0$  when the model predictions are worse than using the mean of the  
 350 observations. Values of  $E'$  for our model indicated a very good fit for soil water content

351 predictions, and an acceptable fit for the total concentration ( $C_s + C_w$ ) predictions for each  
 352 compound, with some close to 0 and a few lower than 0 (Table 3).

353  
 354 **Table 3.** Goodness-of-fit measures for simulations and experimental data. -: non-computed;  $O$ :  
 355 observation;  $\bar{O}$ : mean of observations;  $P$ : predicted value;  $j$ : total number of data points.

Soil core	$\theta$	C12			C14			C16			C18			
		EO3	EO6	EO8	EO3	EO6	EO8	EO3	EO6	EO8	EO3	EO6	EO8	
1	<sup>a</sup> MAE	0.03	1.17	1.57	2.08	0.15	0.67	1.47	-	1.27	-	-	3.83	5.71
	<sup>b</sup> RMSE	0.04	1.35	1.82	3.31	0.22	0.91	2.28	-	1.78	-	-	4.93	7.46
	<sup>c</sup> E'	0.76	-0.59	-0.94	0.02	0.34	-0.16	-0.11	-	-0.20	-	-	0.02	0.25
2	<sup>a</sup> MAE	0.02	-	1.65	8.84	0.14	0.62	0.36	0.15	0.53	0.60	0.12	1.03	4.43
	<sup>b</sup> RMSE	0.02	-	1.98	18.75	0.23	1.29	0.73	0.23	0.63	0.73	0.14	1.61	8.86
	<sup>c</sup> E'	0.68	-	-1.53	-8.18	0.11	-1.23	0.02	-0.02	0.28	0.53	0.31	0.53	0.35

356 <sup>a</sup>Mean absolute error  $MAE = \frac{\sum_{i=1}^j |O-P|}{j}$

357 <sup>b</sup>Root mean square error  $RMSE = \sqrt{\frac{1}{j} \sum_{i=1}^j (O-P)^2}$

358 <sup>c</sup>Modified coefficient of efficiency  $E' = 1 - \frac{\sum_{i=1}^j |O-P|}{\sum_{i=1}^j |O-\bar{O}|}$

359  
 360 **3.2. Sorption isotherms: measured vs. simulated**  
 361 In both batch experiments and numerical simulations, the Freundlich isotherm was the best  
 362 reproducing the sorption process of the AEOs, in agreement with previous studies (Brownawell et  
 363 al., 1997; John et al., 2009). Values of  $K_d$ , describing the coefficient of the sorption isotherm, for  
 364 C12, C14 and C18 from batch experiments ranged from  $1.62 \times 10^{-7}$  to  $1.96 \times 10^{-5}$  cm<sup>3</sup>/ng, while  
 365 values for C16 ranged from  $8.51 \times 10^{-7}$  to  $3.8 \times 10^{-6}$  cm<sup>3</sup>/ng (Figure 4a). In contrast,  $K_d$  values  
 366 obtained from simulations had a narrower range, with values between  $3.72 \times 10^{-8}$  and  $4 \times 10^{-7}$   
 367 cm<sup>3</sup>/ng. When considered as a function of the number of ethoxylated groups, for batch  
 368 experiments, EO3 shows a narrower range than EO6 and EO8, between  $7.47 \times 10^{-7}$  and  $5.89 \times 10^{-7}$   
 369 cm<sup>3</sup>/ng, but, as for carbon chain length, the simulated  $K_d$  value was very similar for all of them  
 370 (Figure 4b). In general, simulated  $K_d$  values were between 1 and 2 orders of magnitude smaller  
 371 than those measured in batch experiments.

372

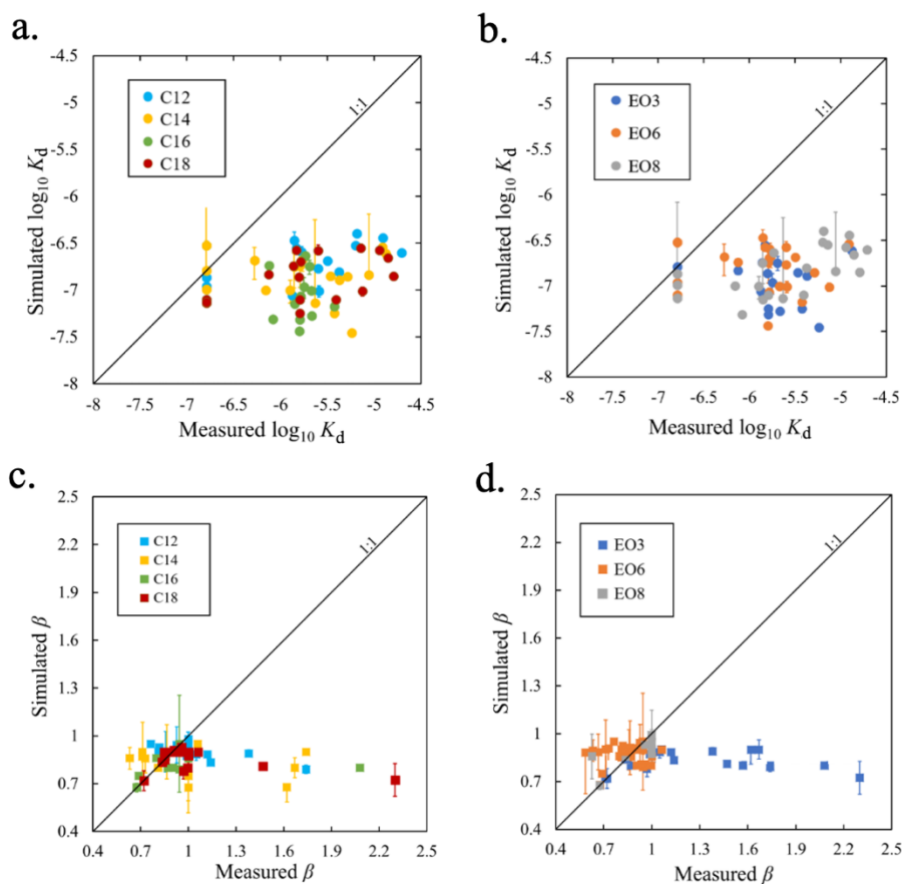


**Figure 4.** (a,b) Values of  $K_d$  [ $\text{cm}^3/\text{ng}$ ] (expressed as  $\log_{10} K_d$ ) from simulation of infiltration experiments plotted against values from batch experiments, with colors representing (a) the length of the carbon chain (C12, blue; C14, yellow; C16, green; and C18, red), and (b) the number of ethoxylated groups (EO3, blue; EO6, orange; and EO8, gray). (c,d) Values of  $\beta$  from simulation of infiltration experiments plotted against values from batch experiments, with colors representing (c) the length of the carbon chain (C12, blue; C14, yellow; C16, green; and C18, red), and (d) the number of ethoxylated groups (EO3, blue; EO6, orange; and EO8, gray). Error bars indicate 95% confidence intervals for the calibrated parameters.

373  
 374 Values of  $\beta$  obtained from batch experiments as a function of the length of the carbon chain range  
 375 from 0.6 to 2, while those from the simulations range from 0.6 to 0.95 (Figure 4c). Overall, similar  
 376  $\beta$  values were obtained from batch experiments and simulation of the infiltration experiments,  
 377 although there were deviations from the line 1:1, most noticeable for values for ethoxymers with  
 378 3 EO groups (Figure 4d) derived from batch experiments.  
 379



### 3.3. Dependence of $K_d$ on clay and organic carbon

A dependence of sorption on the soil clay and organic carbon content has been reported in previous works (Yun-Hwei, 2000; Traverso-Soto et al., 2014), with the following relationships: (i) sorption increases with the number of ethoxylated groups as clay content increases, and (ii) sorption increases with the carbon chain length as organic carbon content increases. In our batch experiments, in contrast, there was an almost stable  $K_d$  value of around  $4 \times 10^{-6} \text{ cm}^3/\text{ng}$  for clay content  $> 1\%$ , regardless of the number of ethoxylated groups (Figure 5a). Similarly,  $K_d$  values reached an asymptote of  $3.16 \times 10^{-6} \text{ cm}^3/\text{ng}$  for organic carbon content  $> 0.3\%$ , regardless of the carbon chain length (Figure 5b). An almost constant value of  $K_d$  as function of clay and organic carbon content, although of lower magnitude, was observed for the simulated values ( $K_d \sim 1 \times 10^{-7} \text{ cm}^3/\text{ng}$ ).

391

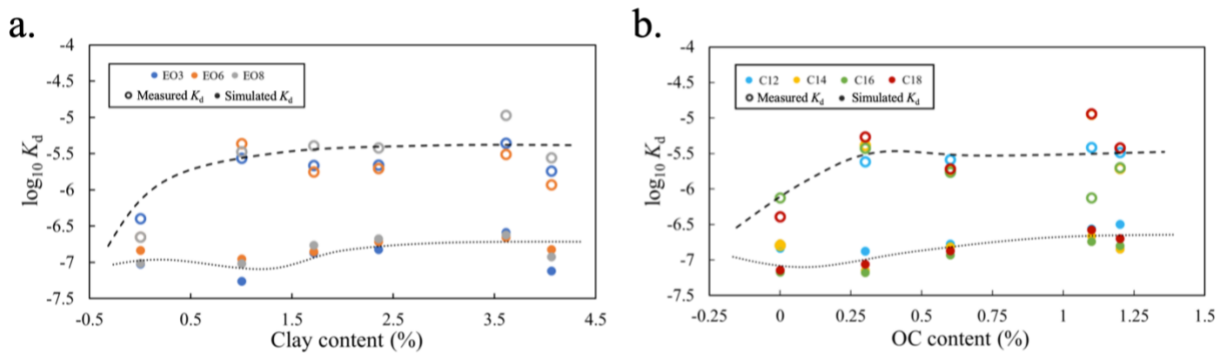


**Figure 5.** (a) Average  $\log_{10} K_d$  values measured in batch experiments (empty circles) and simulated from the infiltration experiments (filled circles) as a function of clay content (%), plotted according to the number of ethoxylated groups: EO3 (blue), EO6 (orange) and EO8 (gray). (b) Average  $\log_{10} K_d$  values measured in batch experiments (empty circles) and simulated from the infiltration experiments (filled circles) as a function of organic carbon content (OC %), plotted according to the carbon chain length: C12 (blue), C14 (yellow), C16 (green) and C18 (red). The dashed and dotted lines represent the moving average for batch and simulated  $K_d$  values, respectively.

392

## 393 4. Discussion

394

395 The direct flow model, *i.e.*, using hydraulic parameters estimated from ROSETTA, captured well  
396 the hydrodynamics in both infiltration experiments. A calibration by inverse method of the

397 hydraulic parameters (using the available water content measurements) did not improve the fit.  
398 This, along with the plausibility of the model parameters, indicated the appropriateness of the flow  
399 parameterization (Figure 2). To assess the appropriateness of the adopted transport-related  
400 parameters, a sensitivity analysis for the dispersivity values taken from the literature  
401 (Vanderborght and Vereecken, 2007) demonstrated the low impact on the conservative and  
402 reactive transport results. Note that the ranges of dispersivity values used were smaller than one  
403 order of magnitude due to the thickness of the soil horizons and the numerical spatial discretization  
404 adopted.

405  
406 HYDRUS-1D (Šimůnek et al., 2015) has been extensively used to solve sorption and the coupled  
407 transport in pore domains with different advective velocities, providing accurate simulations when  
408 compare with a number of numerical models (Vanderborght et al., 2005). The reactive transport  
409 model was based on the flow and conservative transport parameterization. In this case, the inverse  
410 method was used to characterize the sorption process for each surfactant under flow experimental  
411 conditions. Note that, due to the low concentrations used, the impact of surfactants on the hydraulic  
412 properties was discarded (*e.g.*, Kanokkarn et al., 2017). The kinetics of sorption and degradation  
413 (Table 2) were preestablished based on laboratory determinations and literature, respectively.  
414 Sorption kinetics (first order sorption rate coefficient) determined experimentally resulted very  
415 similar to previous estimations for similar compounds. The degradation constant values used (from  
416 Hermens and Droge, 2009) were slightly higher than the ones provided for similar compounds  
417 (*e.g.*, linear alcohol ethoxylates) and for a large variety of soils (Knaebel et al., 1990; Federle et  
418 al., 1997). This resulted in a slightly shorter half-life, *i.e.*, faster decay, which was expected in our  
419 soils as they have been previously exposed to surfactants and other sewage derived chemicals, and  
420 the microbial community might be already acclimated to this type of contaminants. Similar to the  
421 water flow model, the performance of the calibrated model was evaluated both in terms of  
422 goodness-of-fit to available total concentration (sorbed + dissolved) measurements and plausibility  
423 of the model parameters. Although the fit of the model for each surfactant was not as good as for  
424 soil water content, the reactive transport model captured quite well the shape of the total  
425 concentration profiles. Important differences between observed and simulated values were,  
426 however, systematically found for the sampling point at the surface (0 cm depth). This point lies  
427 at the interface between the applied water and the soil surface, and generally presents a high total

428 AEO concentration, both experimentally and numerically. This fact evidences the difficulties in  
429 capturing the processes occurring at the atmosphere–soil boundary layer.

430  
431 The obtained parameterization for the sorption process from both batch experiments and  
432 simulation of the infiltration experiments can be explained from the existing heterogeneity in the  
433 fluid flow at pore scale. From the simulation of the infiltration experiments, the fitted parameter  
434  $K_d$  for each surfactant was  $\sim 1.5$  orders of magnitude smaller than the values obtained from batch  
435 experiments (Travero-Soto et al., 2014). During the initial imbibition phase no fingering (unstable  
436 flow) was observed. However, once steady-state conditions were reached, unsaturated flow in soil  
437 is still very heterogeneous, with the coexistence of high velocity regions (preferential paths) and  
438 low velocity regions or stagnation zones (De Gennes 1983; Jiménez-Martínez et al., 2015, 2017).  
439 This double flow structure (Holzner et al., 2015) reduces the surface contact between the  
440 contaminant and the solid particles, and therefore reduces the sorption capacity. For the other  
441 Freundlich isotherm parameter,  $\beta$ , there was much less discrepancy between estimates from batch  
442 experiments and simulated results from the infiltration experiments, with the exception of values  
443 for the EO3 AEOs, for which the measured range from batch experiments was wider than the  
444 simulated one. The  $\beta$  values (systematically  $< 1$ ) of the adopted Freundlich isotherm, obtained  
445 from the simulation of the infiltration experiments, indicate an agreement with previous studies  
446 where the sorption of non-inonic surfactants in soils was described by a Langmuir isotherm (Lee  
447 et al., 2005). The low concentrations used in the infiltration experiments impeded to reach the  
448 sorption saturation. Note that Freundlich isotherms have also been determined for AEOs in other  
449 matrices such as receiving water solids (Van Compernelle et al., 2006). The comparison  
450 established here highlights the inappropriateness of using sorption parameters inferred from batch  
451 experiments in field-scale environmental studies.

452  
453 When comparison was done considering the structural diversity of AEOs, values of  $K_d$  did not  
454 differ according to the carbon chain length, either in the values deduced from the batch experiments  
455 or simulated from the infiltration experiments. By ethoxylated groups,  $K_d$  from batch experiments  
456 using EO3 ethoxymers remained grouped and with a smaller average value, while EO6 and EO8  
457 did not (Figure 4.b), having larger average values. This can be explained by the hydrogen bonding  
458 between EOs and functional groups on various soil components, which is the primary mechanism

459 accounting for the preferential sorption of long EO homologs. Sorption of individual homologs  
460 within a mixture has been found for increasing as EOs number increases (Yuan and Jafvert, 1997).  
461 Consequently, higher values were expected for groups EO6 and EO8 than for EO3. The similar  
462 values observed for the simulated  $K_d$  as a function of both carbon chain length and ethoxymers can  
463 be explained by the low concentrations used in the infiltration experiments and the fast  
464 biodegradation, which can hide these differences. Estimates of  $\beta$  from batch experiments and in  
465 the simulations did not differ according to the length of the carbon chains or the number of  
466 ethoxylated groups, except for the measured value of  $\beta$  for EO3, which had a wider range of values  
467 than for the other ethoxymers. This difference between ethoxymers was not observed in the  
468 simulated  $\beta$  values, which can be equally explained by the lower concentrations used, and specially  
469 measured as sorbed in the infiltration experiments, and hide by the fast biodegradation.

470  
471 It has been demonstrated that the sorption of non-ionic surfactants is proportional to the clay  
472 content unless the soil has a fairly high organic carbon content (Lee et al., 2005), as well as a larger  
473 affinity with organic substances as carbon chain length increases as compared with the number of  
474 ethoxylate groups (McAvoy and Kerr, 2001). For the AEOs studied, no clear dependence of  $K_d$  on  
475 clay content by number of ethoxylated groups and on organic carbon content by carbon chain  
476 length was observed (Yun-Hwei, 2000; Traverso-Soto et al., 2014). Differences existed, however,  
477 between batch experiments and simulated values in the relationship between  $K_d$  values and the two  
478 soil properties. The value of  $K_d$  reached an asymptote for clay content  $> 1\%$ , while simulated  
479 values remained more or less constant independent of the clay content. Similar behavior is  
480 observed for  $K_d$  as function of organic carbon content, with an asymptote above an organic carbon  
481 content of 0.3%. Both clay and organic carbon content of the used soils were relatively low, which  
482 can explain the no clear trend of  $K_d$  values obtained from both batch experiments and simulated  
483 from the infiltration experiments. The low clay and organic carbon content of the studied soils  
484 explains the lack of a strong correlation of sorption capacity with any of these soil properties  
485 (Figure 5). The simultaneous biodegradation of AEOs, as observed for similar surfactants  
486 (Knaebel et al., 1990) under the experimented aerobic conditions, can hide these differences.

487  
488 Of the total mass of each surfactant applied, up to 99% was sorbed and/or degraded, being sorption  
489 the dominant process in the soil core 1 (slow flow conditions), and the lower sorption in the soil

490 core 2 (fast flow conditions) was counterbalance by the significant degradation. Less than 0.5% of  
491 surfactants mass percolated through to the bottom of the flow cell. Although the sorption capacity  
492 is reduced considerably (by more than one order of magnitude) under environmental conditions  
493 with flow, thereby increasing the potential percolation depth, the rapid degradation, including due  
494 to biodegradation (Brownawell et al., 1997; Cano and Dorn, 1996), and the expected thicker  
495 unsaturated zone (more than the height of the flow cell used) minimizes the risk of the  
496 contamination of groundwater bodies by AEOs. Similar results have been obtained for anionic  
497 surfactants (*e.g.*, LAS) from percolation experiments, in which beyond a retention favored by  
498 higher clay and organic carbon contents especially for longer-chain homologs, a significant  
499 biodegradation reduced the deep percolation (Küchler and Schnaak, 1997; Boluda et al., 2010).

500

## 501 **5. Conclusions**

502

503 The methodology we apply here, combining sorption isotherms obtained from batch experiments,  
504 longitudinal distribution profiles for AEO concentrations using infiltration experiments, and  
505 numerical simulations, demonstrate the need to be cautious when using the isotherms obtained  
506 from batch experiments to assess the risk to subsurface environments imposed by non-ionic  
507 surfactants. The resulting  $K_d$  coefficients for non-ionic surfactants under flow/natural conditions,  
508 and inferred from inverse numerical simulations, were 1 to 2 orders of magnitude lower than those  
509 obtained from batch experiments, independently of the homolog (*i.e.*, carbon chain length and the  
510 number of ethoxylated groups). No clear trends for  $K_d$  as a function of clay and organic carbon  
511 content were observed, independently of the homolog. Therefore, further studies with higher  
512 concentration of contaminants, mimicking a punctual source, are recommended in order to better  
513 characterize the fate and transport of non-ionic surfactant homologs, and in particular the impact  
514 of clay and organic carbon content on the sorption process in soils, reducing the uncertainty in  
515 predictive models and the risk of contamination of groundwater bodies.

516

517 **Acknowledgements.** We thank Emiliano M. Gómez (SCCYT UCA) for his technical assistance  
518 with the LC/MS. The work was carried out as part of the CGL 2008-05598 project, funded by the  
519 Spanish Ministry of Science and Technology (CICYT). M.B.E. and J.J.-M. gratefully  
520 acknowledge the Lifelong Learning Programme – Freemover Scholarship (European

521 Commission). J.J.-M. gratefully acknowledges the financial support from the Swiss National  
522 Science Foundation (SNF, grant Nr. 200021\_178986). The authors acknowledge fruitful  
523 discussions about the experiments with J.E. Smith (McMaster University) and about the numerical  
524 simulations with M. Vanclooster (Université Catholique de Louvain). We thank the anonymous  
525 reviewer and the editor whose valuable comments and suggestions help to improve the manuscript.

526

## 527 **Bibliography**

528 Ahel, M., Schaffner, C., Giger, W. (1996) Behaviour of alkylphenol polyethoxylate surfactants in  
529 the aquatic environment-III. Occurrence and elimination of their persistent metabolites during  
530 infiltration of river water to groundwater. *Water Res.*, 30(1), 37-46.

531 Bear, J. (1972) Dynamics of Fluids in Porous Media. New York: Dover Publications, Inc.

532 Boluda-Botella, N., León, V.M., Cases, V., Gomis, V., Prats, D. (2010) Fate of linear alkylbenzene  
533 sulfonate in agricultural soil columns during inflow of surfactant pulses. *J. Hydrol.*, 395(3-4),  
534 141-152.

535 Biel-Maeso, M., Corada-Fernández, C., Lara-Martín, P.A. (2017) Determining the distribution of  
536 pharmaceutically active compounds (PhACs) in soils and sediments by pressurized hot water  
537 extraction (PHWE). *Chemosphere*, 185, 1001-1010.

538 Brownawell, B.J., Chen, H., Zhang, W., Westall, J.C. (1997) Sorption of nonionic surfactants on  
539 sediment materials. *Environ. Sci. Technol.*, 31(6), 1735-1741.

540 Cano, M. and Dorn, P. (1996) Sorption of two model alcohol ethoxylate surfactants to sediments.  
541 *Chemosphere*, 33(6), 981-94.

542 Carlsen, L., Metzton, M.B., Kjelsmark, J. (2002) Linear alkylbenzene sulfonates (LAS) in the  
543 terrestrial environment. *Sci. Total Environ.*, 290(1-3), 225-230.

544 Connors, K.A. (1990) Chemical kinetics: the study of reaction rates in solution. John Wiley &  
545 Sons.

546 Corada-Fernández, C., Candela, L., Torres-Fuentes, N., Pintado-Herrera, M.G., Paniw, M.,  
547 González-Mazo, E. (2017) Effects of extreme rainfall events on the distribution of selected  
548 emerging contaminants in surface and groundwater: The Guadalete River basin (SW, Spain).  
549 *Sci. Total Environ.*, 605, 770-783.

550 Corada-Fernández, C., Jiménez-Martínez, J., Candela, L., González-Mazo, E., Lara-Martín, P.A.,  
551 (2015) Occurrence and spatial distribution of emerging contaminants in the unsaturated zone.  
552 Case study: Guadalete River basin (Cadiz, Spain). *Chemosphere*, 119, S131-S137.

553 Corada-Fernández, C., Lara-Martín, P.A., Candela, L., González-Mazo, E. (2011) Tracking  
554 sewage derived contamination in riverine settings by analysis of synthetic surfactants. *J.*  
555 *Environ. Monitor.*, 13(7), 2010-2017.

556 Corada-Fernández, C., Lara-Martín, P.A., Candela, L., González-Mazo, E. (2013) Vertical  
557 distribution profiles and diagenetic fate of synthetic surfactants in marine and freshwater  
558 sediments. *Sci. Total Environ.*, 461, 568-575.

559 De Gennes, P.G. (1983) Hydrodynamic dispersion in unsaturated porous media. *J. Fluid Mech.*,  
560 136, 189-200.

561 Ding, W.H., Tzing, S.H., Lo, J.H. (1999) Occurrence and concentrations of aromatic surfactants  
562 and their degradation products in river waters of Taiwan. *Chemosphere*, 38(11), 2597-2606.

563 Droge, S.T. and Hermens, J.L. (2007) Nonlinear sorption of three alcohol ethoxylates to marine  
564 sediment: A combined Langmuir and Linear sorption process? *Environ. Sci. Technol.*, 41(9),  
565 3192-3198.

566 Droge, S.T. and Hermens, J.L. (2010) Alcohol ethoxylate mixtures in marine sediment:  
567 Competition for adsorption sites affects the sorption behaviour of individual homologues.  
568 *Environ. Poll.*, 158(10), 3116-3122.

569 Droge, S.T., Yarza-Irusta, L., Hermens, J.L. (2009) Modeling nonlinear sorption of alcohol  
570 ethoxylates to sediment: the influence of molecular structure and sediment properties. *Environ.*  
571 *Sci. Technol.*, 43(15), 5712-5718.

572 Durán-Álvarez, J.C., Sánchez, Y., Jiménez, B., Prado, B. (2014) The transport of three emerging  
573 pollutants through an agricultural soil irrigated with untreated wastewater. *J. Water Reuse*  
574 *Desal.*, 4(1), 1-9.

575 Eadsforth, C.V., Sherren, A.J., Selby, M.A., Toy, R., Eckhoff, W.S., McAvoy, D.C., Matthijs, E.,  
576 (2006) Monitoring of environmental fingerprints of alcohol ethoxylates in Europe and Canada.  
577 *Ecotox. Environ. Safe.*, 64(1), 14-29.

578 Eichhorn, P., Silvana V. Rodrigues, S.V., Baumann, W., Knepper, T.P. (2002) Incomplete  
579 degradation of linear alkylbenzene sulfonate surfactants in Brazilian surface waters and pursuit  
580 of their polar metabolites in drinking waters. *Sci. Total Environ.*, 284(1-3), 123-134.

581 El Rayis, O. (1985) Re-assessment of the titration method for determination of organic carbon in  
582 recent sediments. *Rapp. Comm. Int. Mer. Medit.*, 29, 45-47.

583 El-Kadi, A.I. and Ling, G. (1993) The Courant and Peclet number criteria for the numerical  
584 solution of the Richards equation. *Water Resour. Res.*, 29(10), 3485-3494.

585 Federle, T.W., Gasior, S.D. and Nuck, B.A. (1997) Extrapolating mineralization rates from the  
586 ready CO<sub>2</sub> screening test to activated sludge, river water, and soil. *Environ. Toxicol. Chem.*,  
587 16(2), 127-134.

588 Ferguson, P.L., Iden, C.R., Brownawell, B.J. (2001) Distribution and fate of neutral alkylphenol  
589 ethoxylate metabolites in a sewage-impacted urban estuary. *Environ. Sci. Technol.*, 35(12),  
590 2428-2435.

591 Garcia, R.A., Chiaia-Hernández, A.C., Lara-Martín, P.A., Loos, M., Hollender, J., Oetjen, K.,  
592 Higgins, C.P., Field, J.A. (2019) Suspect screening of hydrocarbon surfactants in AFFFs and  
593 AFFF-contaminated groundwater by high resolution mass spectrometry. *Environ. Sci.*  
594 *Technol.* 53, 14, 8068-8077.

595 Gaudette, H., Flight, W., Torner, L., Folger, D.W. (1974) An inexpensive titration method for the  
596 determination of organic carbon in recent sediments. *J. Sediment. Res.*, 44(1), 249-253.

597 Gee, G. and Or, D. (2002) Particle size analysis. Methods of soil analysis. Volume Part 4, SSSA  
598 Book Series: 5, Am. Soc. Agron., Madison, WI., pp. 255-294.

599 González-Mazo, E., Forja, J.M., Gómez-Parra, A. (1998) Fate and distribution of linear  
600 alkylbenzene sulfonates in the littoral environment. *Environ. Sci. Technol.*, 32(11), 1636-1641.

601 González-Mazo, E., León, V.M., Sáez, M., Gómez-Parra, A. (2002) Occurrence and distribution  
602 of linear alkylbenzene sulfonates and sulfophenylcarboxylic acids in several Iberian littoral  
603 ecosystems. *Sci. Total Environ.*, 288(3), 215-226.

604 Grossman, R.B. and Reinsch, T. (2002) Bulk density and linear extensibility. Methods of soil  
605 analysis, Volume Part 4, SSSA Book Series: 5, Am. Soc. Agron., Madison, WI., pp. 201-228.

606 Guang-Guo, Y. (2006) Fate, behavior and effects of surfactants and their degradation products in  
607 the environment. *Environ. Int.*, 32(3), 417-431.

608 Haigh, S.D. (1996) A review of the interaction of surfactants with organic contaminants in soil.  
609 *Sci. Total Environ.*, 185(1-3), 161-170.



610 Hermens, J.L. and Droge, S.T. (2009) Human and Environmental Risk Assessment on ingredients  
611 of European household cleaning products, HERA. Alcohol ethoxylates (AEOs). pp. 1-14.  
612 Brussels, Belgium.

613 Holzner, M., Morales, V.L., Willmann, M., Dentz, M. (2015) Intermittent Lagrangian velocities  
614 and accelerations in three-dimensional porous medium flow. *Phys. Rev. E*, doi:  
615 10.1103/PhysRevE.92.013015.

616 Jiménez-Martínez, J., de Anna, P., Tabuteau, H., Turuban, R., Le Borgne, T., Méheust, Y. (2015)  
617 Pore scale mechanisms for the enhancement of mixing in unsaturated porous media and  
618 implications for chemical reactions. *Geophys. Res. Lett.*, 42(13), 5316-5324.

619 Jiménez-Martínez, J., Le Borgne, T., Tabuteau, H., Méheust, Y. (2017) Impact of saturation on  
620 dispersion and mixing in porous media: photo-bleaching pulse injection experiments and  
621 shear-enhanced mixing model. *Water Resour. Res.*, 53(2), 1457-1472.

622 John, D.M., House, W.A., White, G.F. (2009). Environmental fate of nonylphenol ethoxylates:  
623 Differential adsorption of homologs to components of river sediment. *Environ. Toxicol. Chem.*,  
624 19(2), 293-300.

625 Jonkers, N., Laane, R.W., de Voogt, P. (2003) Fate of nonylphenol ethoxylates and their  
626 metabolites in two Dutch estuaries: evidence of biodegradation in the field. *Environ. Sci.*  
627 *Technol.*, 37(2), 321-327.

628 Kanokkarn, P., Shiina, T., Santikunaporn, M., Chavadej, S. (2017) Equilibrium and dynamic  
629 surface tension in relation to diffusivity and foaming properties: effects of surfactant type and  
630 structure. *Colloid. Surf. A Physicochem. Eng. Asp.*, 524, 135-142.

631 Kiewiet, A., de Beer, K.G.M., Parsons, J.R., Govers, H.A.J. (1996) Sorption of linear alcohol  
632 ethoxylates on suspended sediment. *Chemosphere*, 32(4), 675-80.

633 Knaebel, D.B., Vestal, J.R. and Federle, T.W. (1990) Mineralization of linear alkylbenzene  
634 sulfonate (LAS) and linear alcohol ethoxylate (LAE) in 11 contrasting soils. *Environ. Toxicol.*  
635 *Chem.*, 9(8), 981-988.

636 Küchler, T. and Schnaak, W. (1997) Behaviour of linear alkylbenzene sulphonates (LAS) in sandy  
637 soils with low amounts of organic matter. *Chemosphere*, 35(1-2), 153-167.

638 Lara-Martin, P.A., Gómez-Parra, A., González-Mazo, E. (2006) Development of a method for the  
639 simultaneous analysis of anionic and non-ionic surfactants and their carboxylated metabolites

640 in environmental samples by mixed-mode liquid chromatography–mass spectrometry. *J.*  
641 *Chromatogr. A*, 1137(2), 188-197.

642 Lara-Martín, P.A., Gómez-Parra, A., González-Mazo, E. (2008) Sources, transport and reactivity  
643 of anionic and non-anionic surfactants in several aquatic ecosystems from SW of Spain: a  
644 comparative study. *Environ. Pollut.*, 156(1), 36-45.

645 Lara-Martín, P.A., Gómez-Parra, A., González-Mazo, E. (2005) Determination and distribution of  
646 alkyl ethoxysulfates and linear alkylbenzene sulfonates in coastal marine sediments from the  
647 Bay of Cadiz (southwest of Spain). *Environ. Toxicol. Chem.*, 24(9), 2196-2202.

648 Lara-Martín, P.A., González-Mazo, E., Brownawell, B.J. (2011) Multi-residue method for the  
649 analysis of synthetic surfactants and their degradation metabolites in aquatic systems by liquid  
650 chromatography–time-of-flight-mass spectrometry. *J. Chromatogr. A*, 1218(30), 4799-4807.

651 Lara-Martín, P.A., González-Mazo, E., Brownawell, B.J. (2012) Environmental analysis of  
652 alcohol ethoxylates and nonylphenol ethoxylate metabolites by ultra-performance liquid  
653 chromatography–tandem mass spectrometry. *Anal. Bional. Chem.*, 402(7), 2359-2368.

654 Lara-Martín, P.A., González-Mazo, E., Petrovic, M., Barceló, D., Brownawell, B.J. (2014)  
655 Occurrence, distribution and partitioning of nonionic surfactants and pharmaceuticals in the  
656 urbanized Long Island Sound Estuary (NY). *Mar. Pollut. Bull.*, 85(2), 710-719.

657 Lee, J.F., Liao, P.M., Kuo, C.C., Yang, H.T., Chiou, C.T. (2000) Influence of a nonionic surfactant  
658 (Triton X-100) on contaminant distribution between water and several soil solids. *J. Colloid.*  
659 *Interface Sci.*, 229(2), 445-452.

660 Lee, J.F., Hsu, M.H., Lee, C.K., Chao, H.P., Chen, B.H. (2005) Effects of soil properties on  
661 surfactant adsorption. *J. Chin. Inst. Eng.*, 28(2), 375-379.

662 Legates, D.R. and McCabe, G.J. (1999) Evaluating the use of “goodness-of-fit” measures in  
663 hydrologic and hydroclimatic model validation. *Water Resour. Res.*, 35, 233-241.

664 León, V.M., González-Mazo, E., Pajares, J.M.F., Gómez-Parra, A. (2001) Vertical distribution  
665 profiles of linear alkylbenzene sulfonates and their long-chain intermediate degradation  
666 products in coastal marine sediments. *Environ. Toxicol. Chem.*, 20(10), 2171-2178.

667 Matthijs, E., Holt, M.S., Kiewiet, A., Rijs, G.B. (1999) Environmental monitoring for linear  
668 alkylbenzene sulfonate, alcohol ethoxylate, alcohol ethoxy sulfate, alcohol sulfate, and soap.  
669 *Environ. Toxicol. Chem.*, 18(11), 2634-2644.

670 McAvoy, D.C., Dyer, S.D., Fendinger, N.J., Eckhoff, W.S., Lawrence, D.L., Begley, W.M. (1998)  
671 Removal of alcohol ethoxylates, alkyl ethoxylate sulfates, and linear alkylbenzene sulfonates  
672 in wastewater treatment. *Environ. Toxicol. Chem.*, 17(9), 1705-1711.

673 McAvoy, D.C. and Kerr, K.M. (2001) Association of alcohol ethoxylates with a dissolved humic  
674 substance. *Humic substances and chemical contaminants*, Editor(s): C.E. Clapp, M.H.B.  
675 Hayes, N. Senesi, P.R. Bloom, P.M. Jardine. Book Series: ASA, CSSA, and SSSA Books, 177-  
676 186.

677 McAvoy, D.C., White, C.E., Moore, B.L. and Rapaport, R.A. (1994) Chemical fate and transport  
678 in a domestic septic system: Sorption and transport of anionic and cationic surfactants.  
679 *Environ. Toxicol. Chem.*, 13(2), 213-221.

680 Millington, R.J. and Quirk, J. (1961) Permeability of porous solids. *T. Faraday Soc.*, 57, 1200-  
681 1207.

682 Montgomery-Brown, J., Drewes, J.E., Fox, P., Reinhard, M. (2003) Behavior of alkylphenol  
683 polyethoxylate metabolites during soil aquifer treatment. *Water Res.*, 37(15), 3672-3681.

684 Morrall, S., Eckhoff, W.S., Evans, A., Cano, M.L., Dunphy, J.C., McAvoy, D.C. (2006) Removal  
685 of alcohol ethoxylates and environmental exposure determination in the United States. *Ecotox.*  
686 *Environ. Safe.*, 64(1), 3-13.

687 Mualem, Y. (1976) Hysteretical models for prediction of the hydraulic conductivity of unsaturated  
688 porous media. *Water Resour. Res.*, 12(6), 1248-1254.

689 Nash, J.E. and Sutcliffe, J.V. (1970) River flow forecasting through conceptual models, part I: a  
690 discussion of principles. *J. Hydrol.*, 10, 282-290.

691 Petrovic, M., Fernández-Alba, A.R., Borrull, F., Marce, R.M., Mazo, E.G., Barceló, D. (2002)  
692 Occurrence and distribution of nonionic surfactants, their degradation products, and linear  
693 alkylbenzene sulfonates in coastal waters and sediments in Spain. *Environ. Toxicol. Chem.*,  
694 21(1), 37-46.

695 Podoll, R.T., Irwin, C.C., Brendlinger, S. (1987) Sorption of water-soluble oligomers on  
696 sediments. *Environ. Sci. Technol.*, 21(6), 562-568.

697 Reynolds, W. and Elrick, D. (2002) Hydraulic Conductivity of Saturated Soils, Constant Head  
698 Method. In: *Methods of Soil Analyses. Physical Methods*, Book Series 5, Soil Science Society  
699 of America, Madison, WI, pp. 697-700.

700 Ritter, A. and Muñoz-Carpena, R. (2013) Performance evaluation of hydrological models:  
701 Statistical significance for reducing subjectivity in goodness-of-fit assessments. *J. Hydrol.*,  
702 480, 33-45.

703 Schaap, M.G., Leij, F.J., van Genuchten, M. Th. (2001) ROSETTA: a computer program for  
704 estimating soil hydraulic parameters with hierarchical pedotransfer functions. *J. Hydrol.*,  
705 251(3-4), 163-176.

706 Šimůnek, J., Van Genuchten, M.Th., Sejna, M. (2015) The HYDRUS-1D Software Package for  
707 Simulating the One-Dimensional Movement of Water, Heat, and Multiple Solutes in Variably-  
708 Saturated Media. Department of Environmental Sciences, University of California Riverside,  
709 Riverside, CA, USA.

710 Smith, J.E. and Gillham, R.W. (1994) The effect of concentration-dependent surface tension on  
711 the flow of water and transport of dissolved organic compounds: A pressure head-based  
712 formulation and numerical model. *Water Resour. Res.*, 30(2), 343-354.

713 Smith, J.E. and Gillham, R.W. (1999) Effects of solute concentration-dependent surface tension  
714 on unsaturated flow: Laboratory sand column experiments. *Water Resour. Res.*, 35(4), 973-  
715 982.

716 Szymanski, A., Wyrwas, B., Lukaszewski, Z. (2003) Determination of non-ionic surfactants and  
717 their biotransformation by-products adsorbed on alive activated sludge. *Water Res.*, 37(2), 281-  
718 288.

719 Topp, E., Metcalfe, C., Edwards, M., Payne, M., Kleywegt, S., Russell, P., Lapen, Gottschall, N.,  
720 (2012) Pharmaceutical and personal care products in groundwater, subsurface drainage, soil,  
721 and wheat grain, following a high single application of municipal biosolids to a field.  
722 *Chemosphere*, 87(2), 194-203.

723 Traveró-Soto, J.M., Brownawell, B.J., González-Mazo, E., Lara-Martín, P.A. (2014) Partitioning  
724 of alcohol ethoxylates and polyethylene glycols in the marine environment: Field samplings  
725 vs laboratory experiments. *Sci. Total Environ.*, 490, 671-678.

726 Tubau, I., Vázquez-Suñé, E., Carrera, J., González, S., Petrovic, M., López de Alda, M.J., Barceló,  
727 D. (2010) Occurrence and fate of alkylphenol polyethoxylate degradation products and linear  
728 alkylbenzene sulfonate surfactants in urban ground water: Barcelona case study. *J. Hydrol.*,  
729 383(1-2), 102-110.

730 Van Compernelle, R., McAvoy, D.C., Sherren, A., Wind, T., Cano, M.L., Belanger, S.E., Dorn,  
731 P.B., Kerr, K.M. (2006) Predicting the sorption of fatty alcohols and alcohol ethoxylates to  
732 effluents and receiving water solids. *Ecotox. Environ. Safe.*, 64(1), 61-74.

733 Vanderborght, J., Kasteel, R., Herbst, M., Javaux, M., Thiéry, D., Vanclooster, M., Mouvet, C.  
734 and Vereecken, H. (2005) A set of analytical benchmarks to test numerical models of flow and  
735 transport in soils. *Vadose Zone J.*, 4(1), 206-221.

736 Van Genuchten, M.Th. (1980) A closed-form equation for predicting the hydraulic conductivity  
737 of unsaturated soils 1. *Soil Sci. Soc. Am. J.*, 44, 892-898.

738 Vanderborght, J. and Vereecken, H. (2007) Review of dispersivities for transport modeling in  
739 soils. *Vadose Zone J.*, 6(1), 29-52.

740 Wind, T., Stephenson, R.J., Selby, M.A., Eadsforth., C.V., Sherren, A.J., Toy, R. (2006)  
741 Determination of the fate of alcohol ethoxylate homologs in a laboratory continuous activated-  
742 sludge unit study. *Ecotox. Environ. Safe.*, 64, 42-60.

743 Yuan, C. and Jafvert, C. T. (1997) Sorption of linear alcohol ethoxylate surfactant homologs to  
744 soils. *J. Cont. Hydrol.*, 28(4), 311-325.

745 Shen, Y.H. (2000) Sorption of non-ionic surfactants to soil: the role of soil mineral composition.  
746 *Chemosphere*, 41(5), 711-716.